The Comparison of Solar-Powered Hydrogen Closed-Cycle System Capacities for Selected Locations

Evgeny Solomin [1,*], Shanmuga Priya Selvanathan [2], Sudhakar Kumarasamy [1,3,4], Anton Kovalyov [1] and Ramyashree Maddappa Srinivasa [2]

[1] Department of Electric Power Stations, Network and Supply Systems, South Ural State University, 76 Prospekt Lenina, 454080 Chelyabinsk, Russia; sudhakar@ump.edu.my (S.K.); alpenglow305@yandex.ru (A.K.)

[2] Department of Chemical Engineering, Manipal Institute of Technology, Manipal Academy of Higher Education, Manipal 576104, India; shan.priya@manipal.edu (S.P.S.); ramyashreems9@gmail.com (R.M.S.)

[3] Faculty of Mechanical and Automotive Engineering Technology, Automotive Engineering Centre, Universiti Malaysia Pahang (UMP), Pekan 26600, Malaysia

[4] Energy Centre, Maulana Azad National Institute of Technology, Bhopal 462003, India

* Correspondence: solominev@susu.ru

Abstract: The exhaustion of fossil fuels causes decarbonized industries to be powered by renewable energy sources and, owing to their intermittent nature, it is important to devise an efficient energy storage method. To make them more sustainable, a storage system is required. Modern electricity storage systems are based on different types of chemical batteries, electromechanical devices, and hydrogen power plants. However, the parameters of power plant components vary from one geographical location to another. The idea of the present research is to compare the composition of a solar-powered hydrogen processing closed-cycle power plant among the selected geographical locations (Russia, India, and Australia), assuming the same power consumption conditions, but different insolation conditions, and thus the hydrogen equipment capacity accordingly. The number of solar modules in an array is different, thus the required hydrogen tank capacity is also different. The comparison of equipment requires building an uninterrupted power supply for the selected geographical locations, which shows that the capacity of the equipment components would be significantly different. These numbers may serve as the base for further economic calculations of energy cost.

Keywords: solar energy; hydrogen; loop cycle; electrolyzer; fuel cell

1. Introduction

Owing to industrialization and exponential population growth, the rate of energy use in the form of fossil fuel has been steadily growing over time [1]. The incremental exhaustion of fossil fuels may lead civilization to the point of having no hydrocarbons. A report states that, in 2014, total global carbon emissions were about 36 billion tons, about 1.6 times the levels in the 1990s [2]. A previous study has suggested that there will be an energy deficit of more than 1000 EJ globally by the end of 2050 [3]. The global carbonized industries are one of the main contributors to atmospheric pollution and global warming. In contrast to the pre-industrial period, the global temperature has risen from 1.5 to 4.5 °C [4]. The fact to be concerned about is the fossil fuel sources currently used, as the main energy source will get exhausted after 200–300 years of their usage. This period is estimated as the gap between the year 1800 when the mass consumption of oil started [5], and the forecast of British Petroleum Company for oil to be exhausted by the year 2070 [6]. Gas and coal reserves data can be retrieved from the same source and will be 50 and 150 years, respectively.

This period is not remarkable, compared with at least the 2000 years of the history of mankind. Martins et al. [7] proved that there will be a depletion of oil, coal, and gas to 14%,

72%, and 18%, respectively, by 2050. It is anticipated that the same situation may also arise in the countries like USA, China [8], Japan, Korea [9], and several other countries in the middle of the 21st century.

For centuries, people were trying to find new and better fuels as alternatives to hydrocarbons, but without groundbreaking success [10]. The idea of using water as the energy carrier is as old as time but came into light in the 20th century with the extraction of hydrogen from it through electrolysis. Green hydrogen appears to be one of the potential uses of renewable energies [11]. Hydrogen is a chemical element that has the highest power capacity and only secondary energy carrier suitable for wider application [12]. Thus, hydrogen can be used as the future fuel which will be almost inexhaustible [13]. In 2005, the Federal government Energy Policy Act also emphasized hydrogen and its importance as an alternate fuel [14]. Since the Paris Agreement on Climate Change in 2015, countries worldwide have taken measures to reduce carbon dioxide levels in the atmosphere [15]. It has been reported that the European Union and the United States also have targets regarding renewable energy resources (RESs) [16]. The European Union's (EU) goals for renewable energy output in 2030, in particular, aimed for a value of 27 percent for renewable energy consumed in the EU that year [17]. Qatar has also shown greater interest in developing renewable energy and has a 10% renewable energy target by 2030 [18]. Considering the fact that unique source of renewable source of energy the world is solar energy and main source of all energy available on earth, [19] Germany has increased its renewable energy from solar and wind power is increasing in Germany, accounted for about 35% of total power production in 2019 [20].

The change from traditional to renewable power sources requires large investments not only in terms of the generation of power but also in terms of making them feasible to use [21]. The environmental issues related to fossil fuel exhaustion has awaken the world [22]. New energy sources that are environmentally friendly and long-lasting have become a research hotspot in the energy sector [23]. Today, hydrogen is considered a prosperous fuel since the time for deposit depletion is estimated to be 50–100 years [24,25]. Only 4% of hydrogen comes from water, typically through electrolysis [26–28]. The main reason for such a disproportion is the large energy consumption compared with modern conversion methods [29,30], and thus the high cost of the end product as estimated [31]. Adding the cost of the expensive equipment, this approach almost reduces to zero as there are more chances of using hydrogen as a main fuel nowadays.

However, the situation may change in the decarbonized future, when hydrogen may be considered as one of the primary fuels [32]. Some researchers consider the autonomous locations to be equipped with renewables and hydrogen fuel cell capacities [33]. However, the driving potential of global energy consumption, which is in the order of 150 Petawatt-hours per year, by hydrogen only is an impracticable goal, and should rather be supported by all available renewable sources such as biofuels and all kinds of renewables [34].

Many researchers try to improve the efficiency of the hydrogen loop cycle and achieved some significant results. M Gül et al. studied hydrogen generation from a small-scale solar photovoltaic thermal (PV/T) electrolyzer system [35], which has application in fields like air PV/T and modules [36–38]. T.Yi et al. carried out an analysis on factors affecting PV power generation in China [39]. A. Nespoli et al. [40] studied the 24 h ahead forecasting performance of two commonly used artificial neural network (ANN)-based methods for the prediction of the power output of photovoltaic systems, which was one of the first of its kind of study in that filed. W. Li et al. [41] in their study analyzed the difficulties of integrating large solar power generation systems with some realistic future perspectives. A. Dolara et al. [42] proposed a new method of data analysis named physical hybrid artificial neural network (PHANN) based on ANN and tested its reliability in forecasting the PV plant power output. Similar studies were carried out by other researchers using different methods of data analysis [43–46]. R. Machel et al. studied different models that describe the behavior of photovoltaic (PV) sources, explaining their importance in power management [47]. N. Bizon et al. [23] stated the importance of the development of the

new approach to energy sustainable development based on hybrid power systems (HPSs) combining renewable energy sources (RESs) and fuel cell (FC) systems. For instance, B. Schouten in his thesis discussed the hydrogen-oxygen combined cycle power plants based on renewables, showing the optimized fuel cell power density [48].

However, the studies on different insolation locations where the solar energy usage on the basis of hydrogen and power production equipment, which plays a vital role of uninterrupted power supplies, are not revealed. Thus, the idea of the present research is to gain an understanding of the ability of solar power generation and determine the PV equipment capacity depending on the geographical location of the selected regions, which are having the same energy consumption.

The specific task is to cover the constant 1 kW power consumption during the whole mean statistical year by PV solar panels in combination with the loop cycle hydrogen-powered power plant, i.e., to simulate the plant using water and solar energy in an electrolyzer for hydrogen production and storage, and fuel cell stack for extraction of power. Normally, the solar panels supply the consumer 1 kW constantly, 24 h a day, and run the electrolyzer. During the nights and cloudy days, the stored hydrogen to be used to cover the deficient power of fuel cells. The task is divided into two sub-tasks:

- To simulate the hybrid photovoltaic-hydrogen power plant (PV-H PP) and determine the number of PV panels in the array for different locations using the Matlab/Simulink package.
- To determine the volume of hydrogen storage tank assuming the same 1 kW constant consumption in each location.

The three locations chosen for the study are Russia, India, and Australia. Locations were selected because of their typical features like—Russia is located in the Northern Hemisphere, Australia is located in the Southern Hemisphere, and India is located close to the Equator. Any other location will be more or less similar to the ones in the selected points in terms of insolation and hydrogen volume requirement accordingly.

2. Methods and Approaches

2.1. Insolation Measurements

2.1.1. Insolation Data for Chelyabinsk, Russia

The data on insolation for the year 2020 in Russia were obtained by a meteorological station located in Chelyabinsk, Russia, as shown in Figure 1. The measurements were carried out every 4 h each day. The simulation was adjusted for 10 s. Because the instantaneous value of solar radiation is known every 4 h, this mean value is taken as constant during the next 4 h, and so on. It reflects some average value. However, the resulting annual solar energy insolation data were verified by the value of monthly and annual cumulative solar radiation [49].
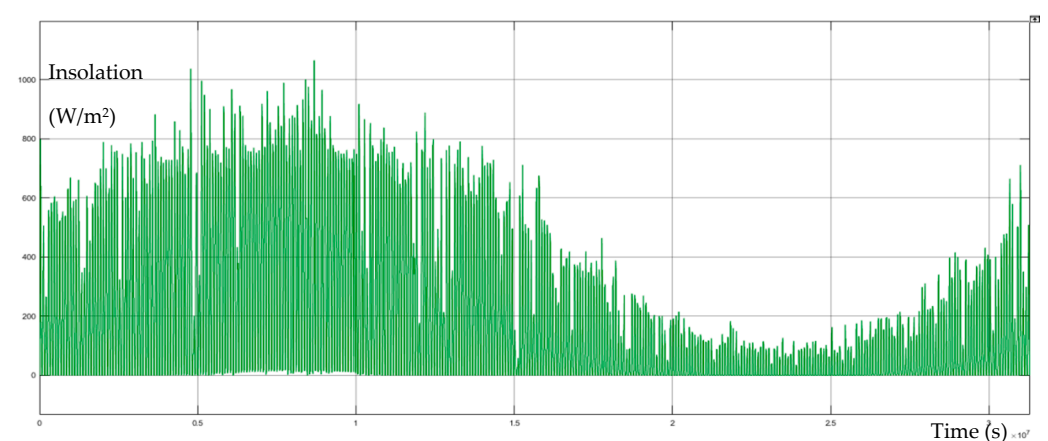

Figure 1. Insolation (W/m^2) in Chelyabinsk city, Russia during the year 2020, starting from April.

2.1.2. Insolation Data for Manipal, India

The solar insolation data for the year 2020 in Manipal, India were obtained based on photovoltaic geographical information system data [50], and is shown in Figure 2. Note: The initial data were presented in the form of mean monthly radiation (kWh/m^2) and then re-calculated into the solar power (W/m^2) as mean daily values, constant from month to month.
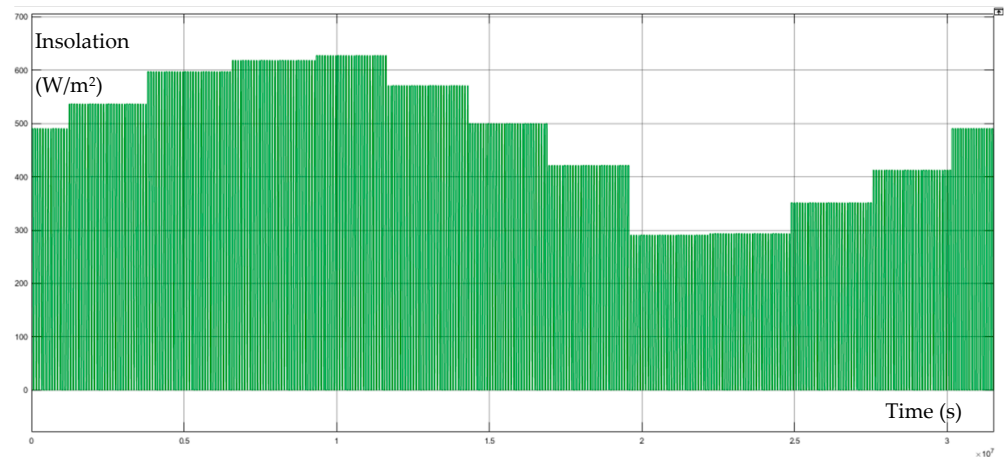

Figure 2. Insolation (W/m^2) in Manipal city, India during the year 2020, starting from April.

2.1.3. Insolation Data for Gnaraloo, Australia

The solar insolation data for the year 2020 in Gnaraloo, Australia were obtained based on open source photovoltaic geographical information system data [50] and are presented in Figure 3.
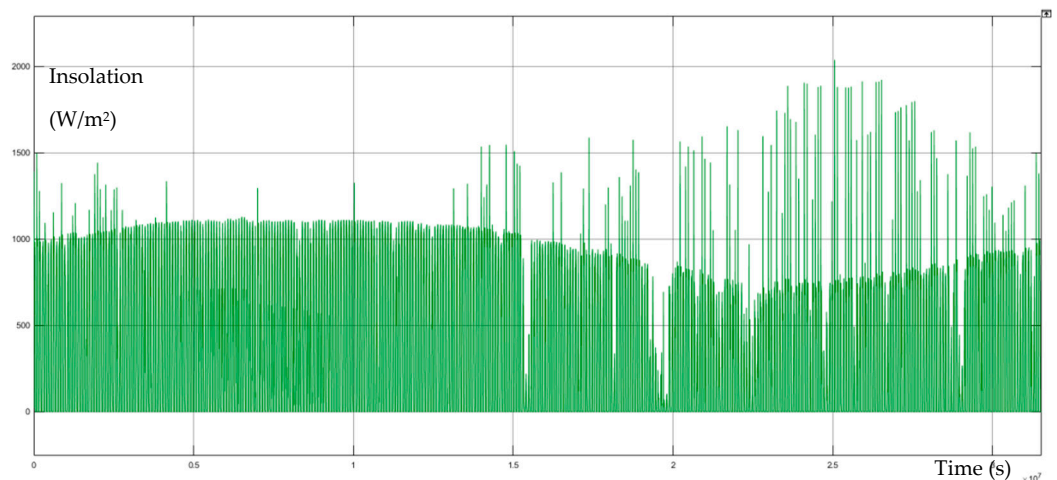

Figure 3. Insolation (W/m^2) in Gnaraloo city, Australia during the year 2020, starting from April.

The approaches of obtaining the instantaneous solar radiation are different, but all give adequate numbers that could be used as the base for simulation.

2.2. The Equipment Parameters Used in the Simulation

2.2.1. Consumer

The consumer is considered as a mean estimated middle class residential or small business entity and assumed constant in all selected locations on the level of 1 kW (1000 W) of constant power consumption, 24 h a day, 7 days a week, 365 days a year. This is the basic point for comparison of the supplying equipment capacity in different plant locations. The further analysis shows that the main idea of the study is to compare the same consumption

for understanding the difference in the support hydrogen equipment capacity, and the rated consumption power can be estimated for all selected points being analyzed.

The presently used power assumption was made based on the following data analyzed by Henrique Pombeiro et al. [51]. The average power consumption for social classes A–C is in general close to, but not exceeding 1 kW [51]. Similar numbers for the mean estimated power consumption for a small business and commercial users (excluding industrial) were also proved by the analysis of commercial small business electricity consumption [52].

2.2.2. Solar Module Array

HVL-360/HJT solar modules are assigned for the round-the-clock supply of the consumer [53]. The solar module consists of solar cells, as shown in Figure 4. Several modules form an array.
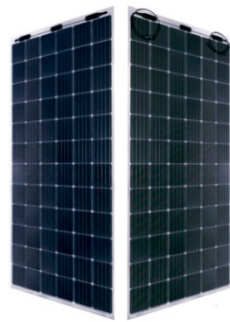

Figure 4. Solar module HVL-360/HJT.

The technical parameters of the module are shown in Table 1.

Table 1. Parameters of the HVL-360/HJT module.

Parameter	Value	Unit
Maximum power	360	W
Dimensions of solar panel	1996 × 1002 × 30	mm
Output operating voltage	50	V
Nominal voltage U_{nom}	43.3	V
Current in nominal point I_{mnp}	8.32	A
Current of short circuit I_{sc}	8.85	A
Voltage of open circuit U_{oc}	52.1	V
Voltage temperature coefficient t_U	−0.239	%/°C
Current temperature coefficient t_I	0.035	%/°C
Number of cells in module	6 × 12 = 72	pcs.

The insolation chart is entered in the Solar Energy Matlab/Simulink model subsystem, as shown in Figure 5.
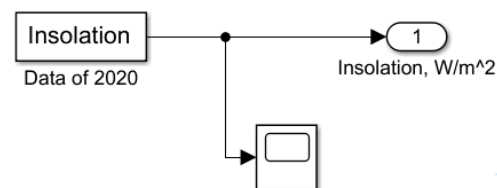

Figure 5. Solar Energy Matlab/Simulink model subsystem.

The scheme of an array of solar modules is presented in the following chart as shown in Figure 6.
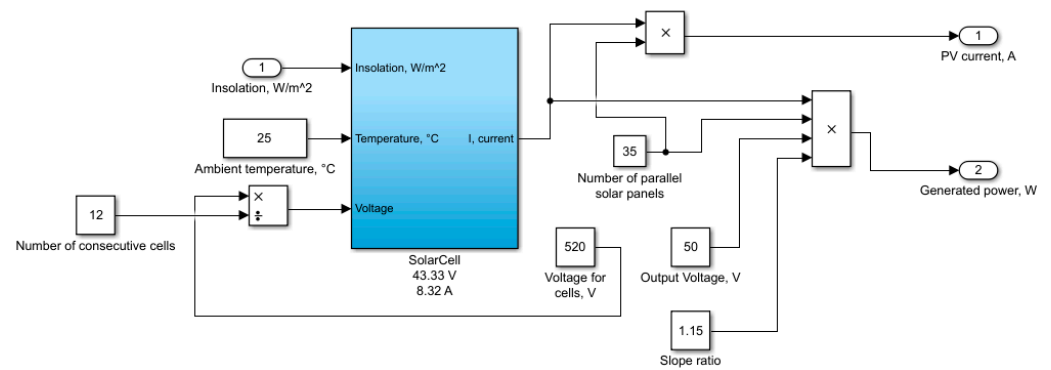
Figure 6. Scheme of an array of solar modules.

2.2.3. Electrolyzer

The VOLTIANA electrolyzer was selected for the simulation [54]. The technical characteristics are presented in Table 2.

Table 2. Parameters of the VOLTIANA electrolyzer.

Parameter	Value	Unit
Capacity, as hydrogen (ref. dry gas)	360	Nm^3/h
Current stack	40–200	A
Voltage stack at 80 °C	48	VDC
Power consumption electric	11	kW

In a simplified form, the subsystem of the electrolyzer in Matlab/Simulink looks as shown in Figure 7, and the subsystem of the electrolyzer cell stack is shown in Figure 8.

The blocks (1/200 s + 1 and 1/100 s + 1) represent the transfer functions for power differences. They are used for smoothing the input values (in this case, simulating the system inertia) to imitate the real system behavior.

The principle of operation is as follows: when there is enough power for the consumer (solar-generated power exceeds 1 kW), the electrolyzer cells will switch on step by step, depending on the amount of power available.

For efficient operation of the plant, the electrolyzer cells must be configured so that the hydrogen production would be proportional to the available power. To achieve that, we entered 44 steps/conditions at 250 W each (11,000 Watt/44 = 250 W). When all conditions are triggered, the maximum output power of 11 kW is generated.
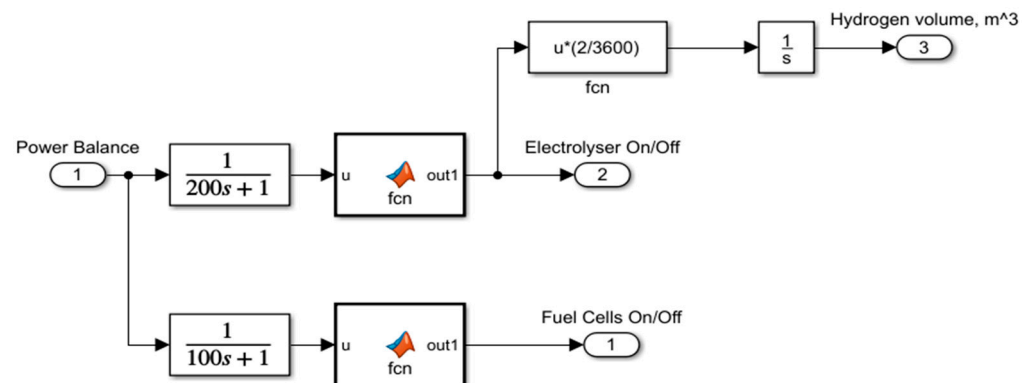

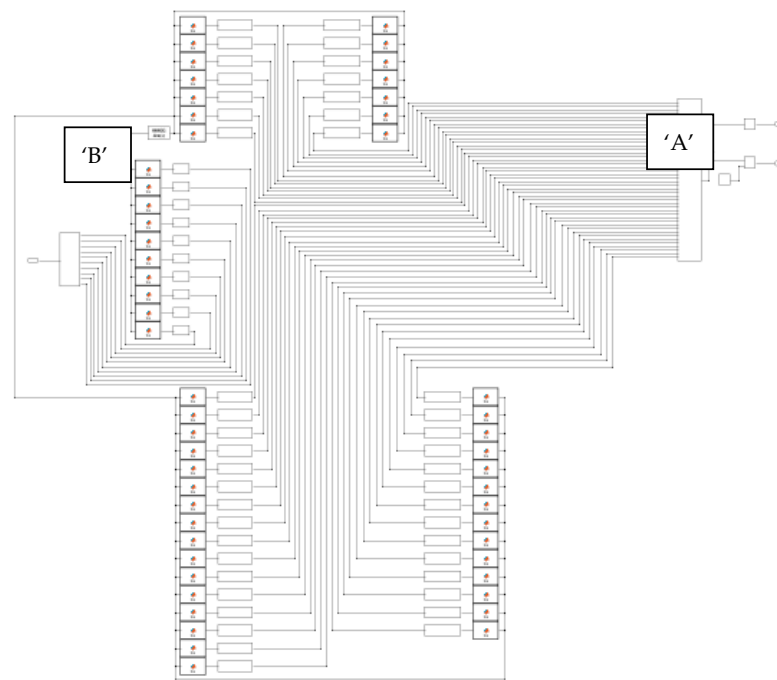**Figure 7.** The subsystem of the electrolyzer.

Figure 8. The subsystem of electrolyzer cell stack (places 'A' and 'B' are shown in the next figures).

The subsystem of the electrolyzer cell stack with A and B input are shown in Figures 9 and 10. The input 'A' receives the power difference (energy output minus consumption). The transfer functions are set up for graph smoothing. The upper 'fcn' block is configured to turn on the electrolyzer at an overall excess of 200 + 100 = 300 W (first and each next step for electrolyzer (200 W) plus power for water pump (100 W)). The output shows "1" when the condition is triggered. Otherwise, the output value tends to zero. Each next power step adds 200 W above the previous one. The maximum rated power consumption of the electrolyzer is 11,000 W. The lower 'fcn' unit is configured for an input power of less than 150 W (100 W is required for the operation of the pump at the fuel cell to pump hydrogen gas from the tank to the fuel cell). The production of hydrogen per hour is divided by 3600 as the entire calculation is carried out in seconds. When the electrolyzer is turned on, the production of hydrogen in cubic meters is activated, which is then pumped to the storage tank. The amount of storage capacity is to be determined.
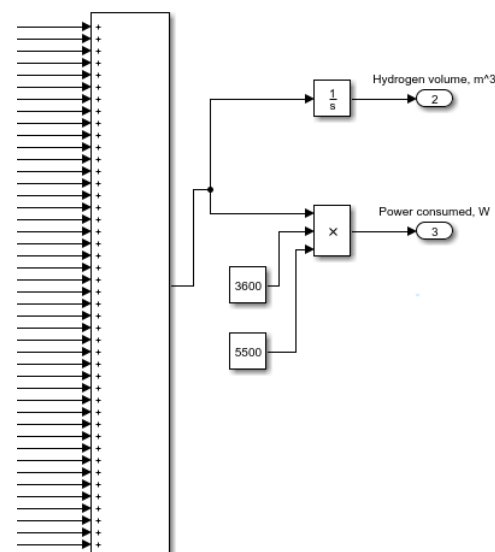

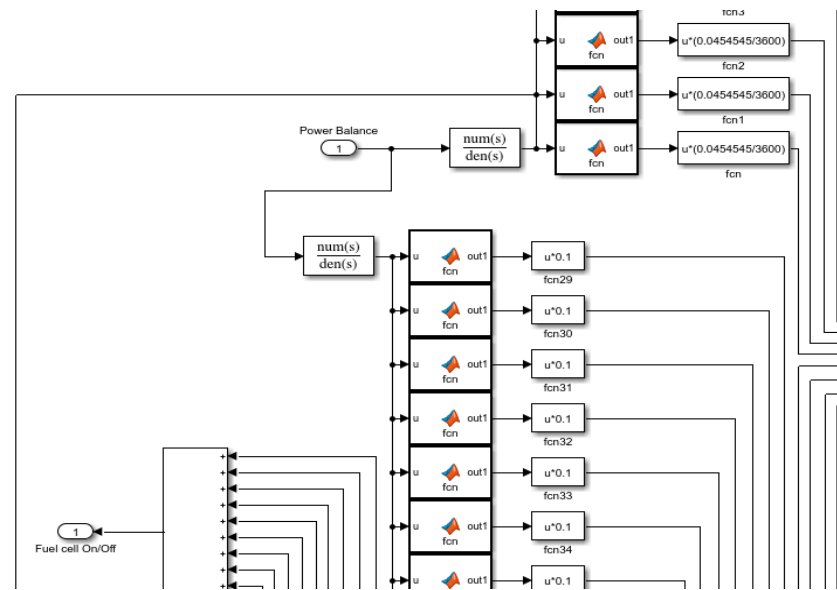**Figure 9.** The subsystem of the electrolyzer cell stack (place 'A').

Figure 10. The subsystem of the electrolyzer cell stack (place 'B').

2.2.4. Fuel Cell

The ultra-light fuel stack AEROSTAK Horizon is selected as a sample for the current research [55] which is shown in Figure 11.

Figure 11. AEROSTAK Horizon fuel cell stack.

The technical specifications of the AEROSTAK Horizon fuel cell stack are shown in Table 3.

Table 3. Parameters of the AEROSTAK Horizon fuel cell stack.

Parameter	Value	Unit
Number of fuel cells	65	pcs
Rated power (and max)	1000 (1300)	W
Reagents	hydrogen and air	
Operating temperature	1–35	°C
Maximum temperature	65	°C
Working pressure of hydrogen	0.5–0.7	Bar
Flow rate of hydrogen: maximum	15.2	L/min
Hydrogen purity requirement	99.999	%

Note: If the power for the fuel cell (FC) is less than 1 kW, it consumes only the amount of hydrogen needed to provide the missing power.

2.2.5. Hydrogen Storage System

When the signal for switching on, the FC is activated, following which activates the corresponding subsystem. A signal equal to "1" is multiplied by the amount of hydrogen consumption and subtracted from the amount of accumulated hydrogen volume. The hydrogen consumption in FC is given in units of L/min. In the FCN block, the value is converted to m^3/s.

The hydrogen storage tank is considered as the thermally isolated system with no weather influence because, in general, there is almost no difference in hydrogen storage equipment for the cold or warm climate, as the H_2 gas density changes in a very small range depending on the temperature [56]. Hydrogen production and pumping for fuel cell operation are shown in Figure 12.
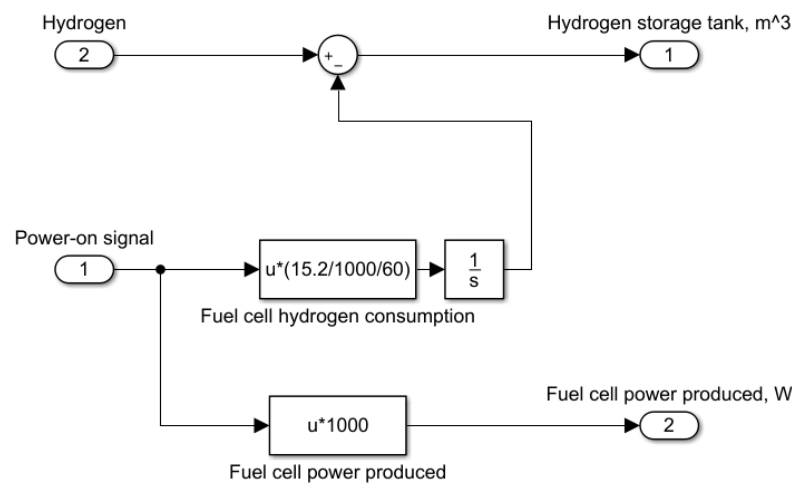

Figure 12. Hydrogen production and pumping for fuel cell operation.

2.2.6. Final Photovoltaic Powered Hydrogen Simulink Model

The complete model of the photovoltaic powered hydrogen generation system in Matlab/Simulink is presented by the following chart, Figure 13.
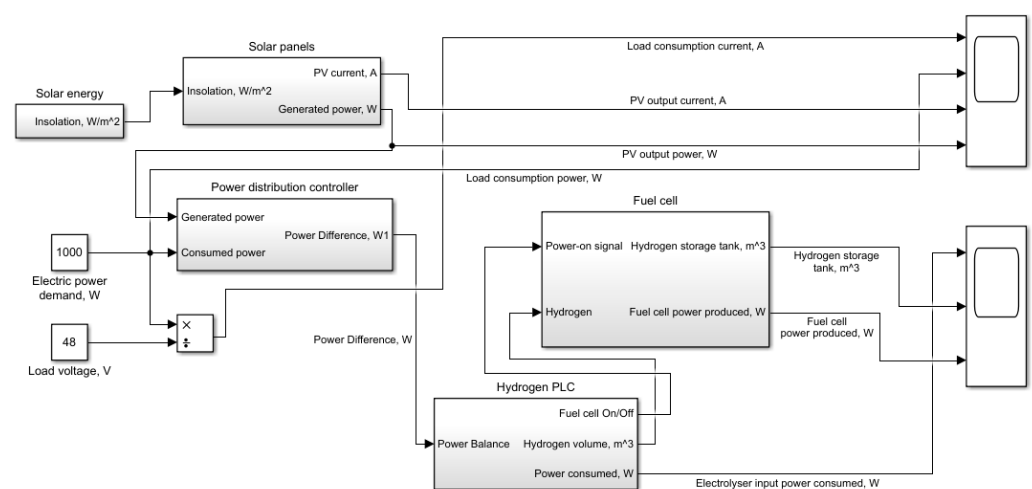

Figure 13. The complete model of the photovoltaic powered hydrogen generation system in Matlab/Simulink.

The calculation is carried out in seconds (the abscissa axis on the graphs below). Accordingly, there are $60 \times 60 \times 24 \times 365$ s in a year. This value is entered in the calculation timeline.

To adjust the whole model and make it maximally adequate, the calibration of the output data is checked, comparing the values of solar module model output in W/m^2 and the alternative constant 1000 W/m^2 input, as shown in Figure 14.
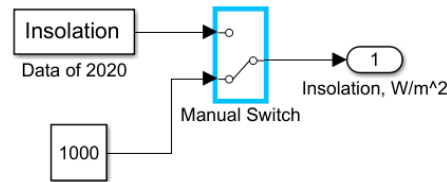

Figure 14. The toggle switches to the corresponding constant in the case of automatic checking of the data.

The solar insolation data were obtained on the horizontal surface. The constant slope of the solar module, equal in the general case to geographic latitude, increases the insolation values by 15% on average. To count this increment, an additional block was added.

The power output by the array of 10 solar modules is shown in Figure 15.

$$P_{array} = P_{module} \cdot N_{module} \cdot K_{slope} = 360 \times 10 \times 1.15 \tag{1}$$

where P_{array}—the power of the solar array; N_{module}—the number of solar modules in an array; P_{module}—the power of one solar module; and K_{slope}—the approximate slope factor, for re-calculation of insolation and/or power from a horizontal surface to the optimal constant slope angle.
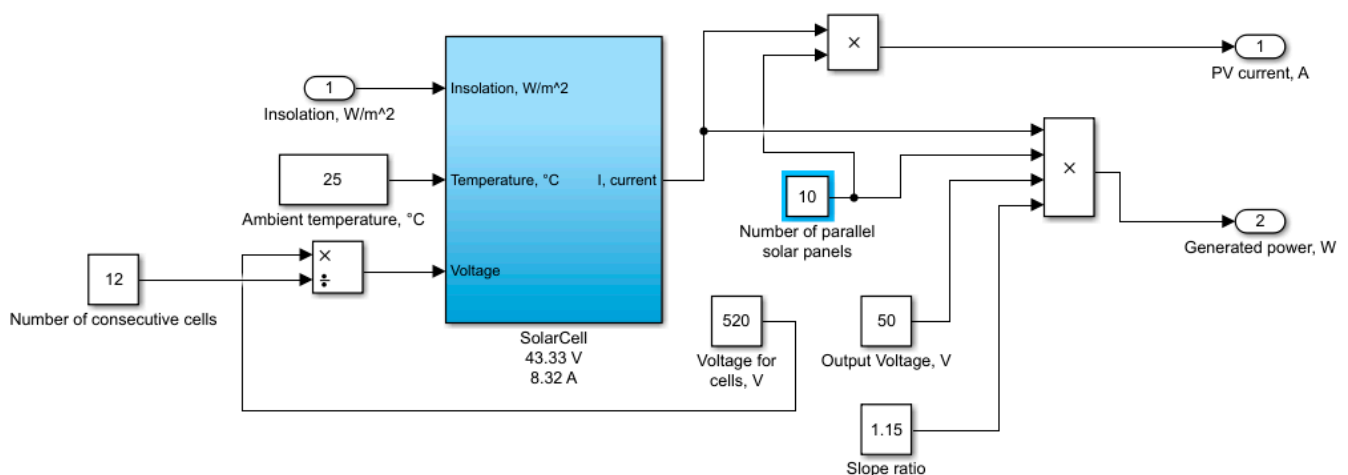

Figure 15. The array of 10 solar modules gives the output power.

Equation (1) shows the power output of solar modules in an array.

2.2.7. Implementation and Safety

The implementation of the equipment similar to the one mentioned was realized in Russia back in 2013. The safety of the real equipment used as a prototype for the simulation was reported E. Solomin [57]. Overall, the safety system counts 11 sensors that block the hydrogen supply in case of any gas leakage, in six places (before and after the electrolyzer, fuel cell stack, and storage tank).

3. Processing Data

The results of the simulation of solar-powered hydrogen generation and utilizing equipment for different locations with different insolation (Russia, India, Australia) are shown in Figures 15–21. The parameters of hydrogen storage in every case are optimized

so that the hydrogen stored volume should be about zero (utilized in full) at the end of the studied year. The model does not contain the servicing time, assuming that it can be done in 1–2 days, which would not influence the overall results.

It is considered that the consumer is the same for all locations as per the estimation made in Section 2.2.1. Consumer, and its consumption everywhere is constant for a better understanding of the difference in the equipment required capacity. The constant consumption parameters (current 20.83 A under 48VDC voltage and power 1 kW) are shown in Figure 16.
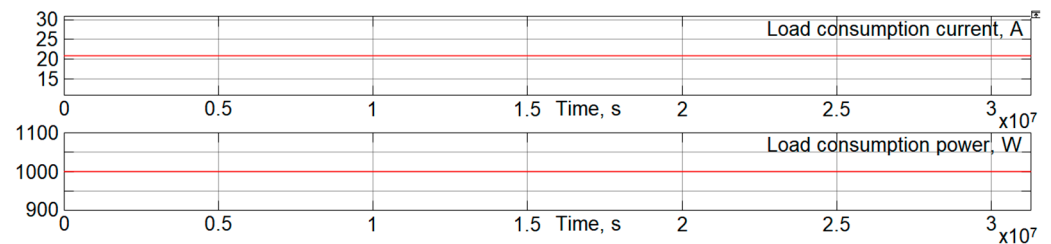

Figure 16. The parameters (current and power) of consumption in each location are equal.

3.1. Simulation Results (Russia)

The result of the calculations for the location Chelyabinsk, Russia is shown in Figure 17.
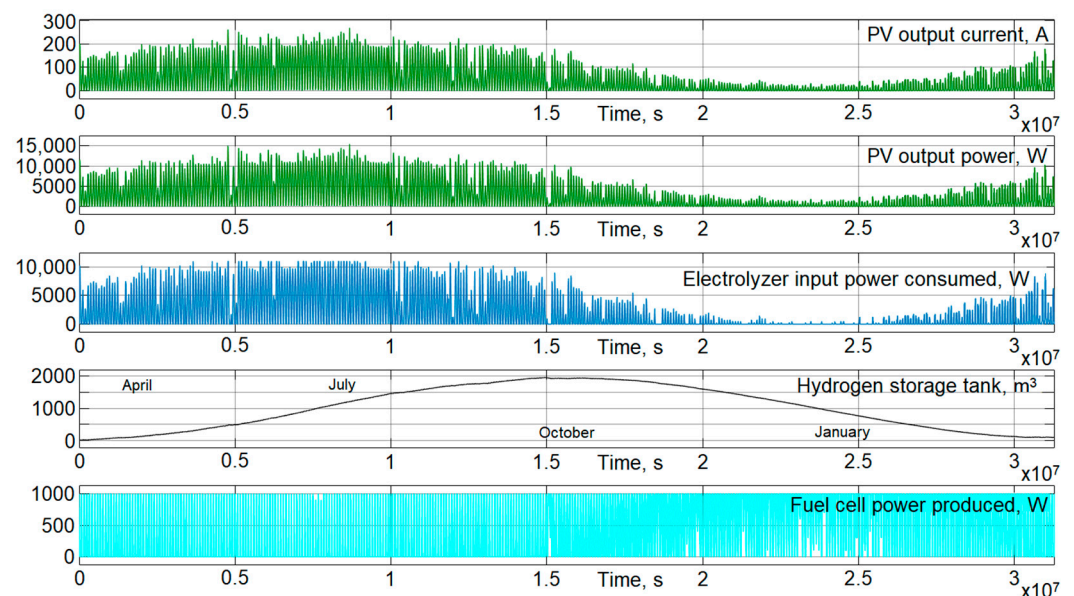

Figure 17. The result of the simulation and calculation of the required hydrogen tank capacity for the location Chelyabinsk, Russia.

The first two graphs display the output current and power of the solar modules array, respectively. The third graph shows the power consumed by the electrolyzer. The fourth graph shows the volume of hydrogen in the tank. This graph allows us to determine the maximum volume of accumulated hydrogen per year in the uncompressed state; the specific tank capacity required for Russia is $\approx$2000 m^3. The lowest fifth graph shows the output power of the fuel cell stack. It operates during no insolation (in the nights, cloudy weather, and so on).

The optimized number of solar modules in an array is 35 pieces. It can be seen from the graphs that the minimal insolation during September to November leads to a significant increase in the hydrogen storage volume ($\approx$2000 m^3).

The optimization of the solar module number in the array in combination with the hydrogen stored volume tending to zero by the end of the year gives a clear understanding of the required equipment parameters.

The following graphs are scaled/zoomed for one month (April) just for a better understanding of energy and hydrogen production.

Figure 18 shows the result of the simulation and calculation of the required hydrogen tank capacity for Chelyabinsk, Russia (April only).

Figure 18. The result of the simulation and calculation of the required hydrogen tank capacity for the location Chelyabinsk, Russia (April only).

3.2. Simulation Results (India)

The result of the calculations for the location Manipal, India is shown below (Figure 19).

Figure 19. The result of the simulation and calculation of the required hydrogen tank capacity for the location Manipal, India.

The first two graphs show the output current and power of the solar modules array, respectively. The third graph shows the power consumed by the electrolyzer. The fourth

graph shows the volume of hydrogen in the storage tank. This graph allows us to determine the maximum volume of accumulated hydrogen per year in the uncompressed state; the tank required capacity is ≈600 m³. This is almost three times less than the tank capacity required for Russia because of lower integral insolation. The lowest fifth graph shows the output power of the fuel cell stack. Again, they operate similar to Russian equipment during no or lack of sunlight.

The optimized number of solar modules in an array is 32 pieces. The following graphs are scaled for the one month (April) just for a better understanding of the energy and hydrogen production, as shown in Figure 20.
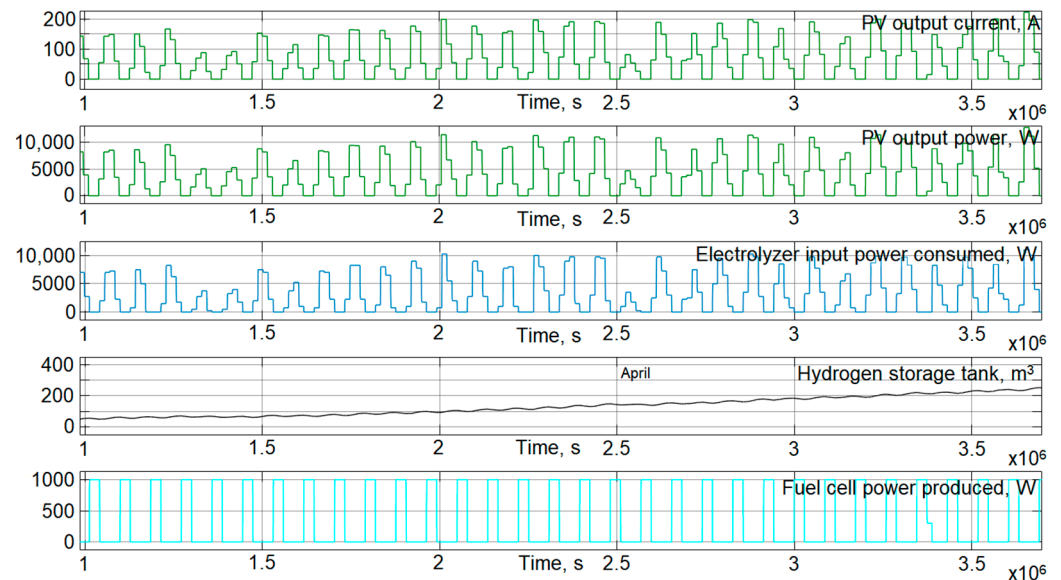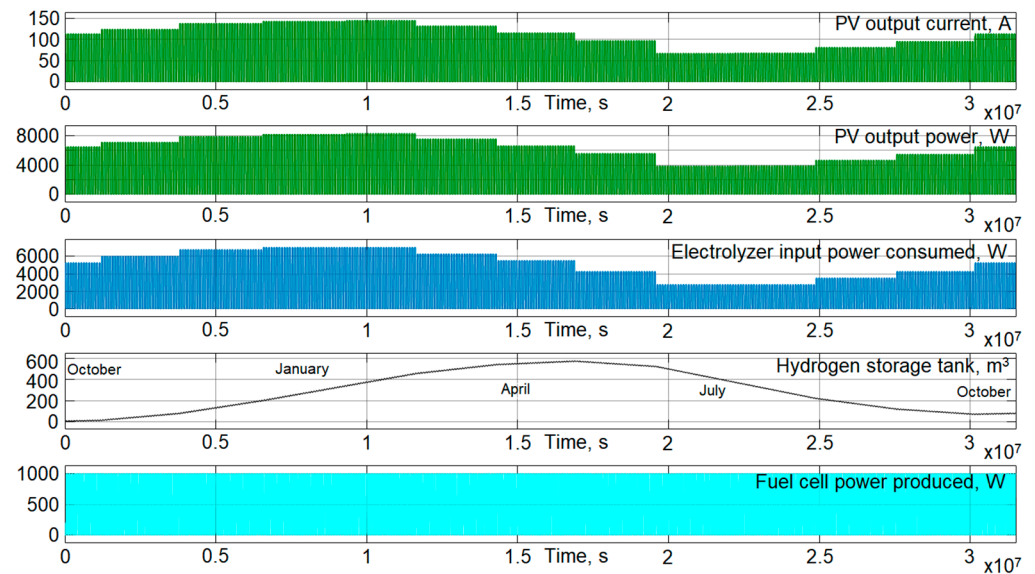

Figure 20. The result of the simulation and calculation of the required hydrogen tank capacity for the location Manipal, India (April only).

3.3. Simulation Results (Australia)

The result of the calculations for the location Gnaraloo (Cape Cuvier), Australia is shown in Figure 21.

Figure 21. The result of the simulation and calculation of the required hydrogen tank capacity for the location Gnaraloo, Australia.

The first two graphs show the output current and power of the solar modules array, respectively. The third graph shows the power consumed by the electrolyzer. The fourth graph shows the volume of hydrogen in the tank. This graph allows us to determine the maximum volume of accumulated hydrogen per year in the uncompressed state. The tank required capacity is $\approx$800 m^3. This is almost two times less than that tank capacity required for Russia, but about 30% higher than that of India. The lowest fifth graph shows the output power of the fuel cell stack.

The optimized number of solar modules in an array is 23 pieces. The following graphs are scaled for the one month (April) just for a better understanding of the energy and hydrogen production (Figure 22).
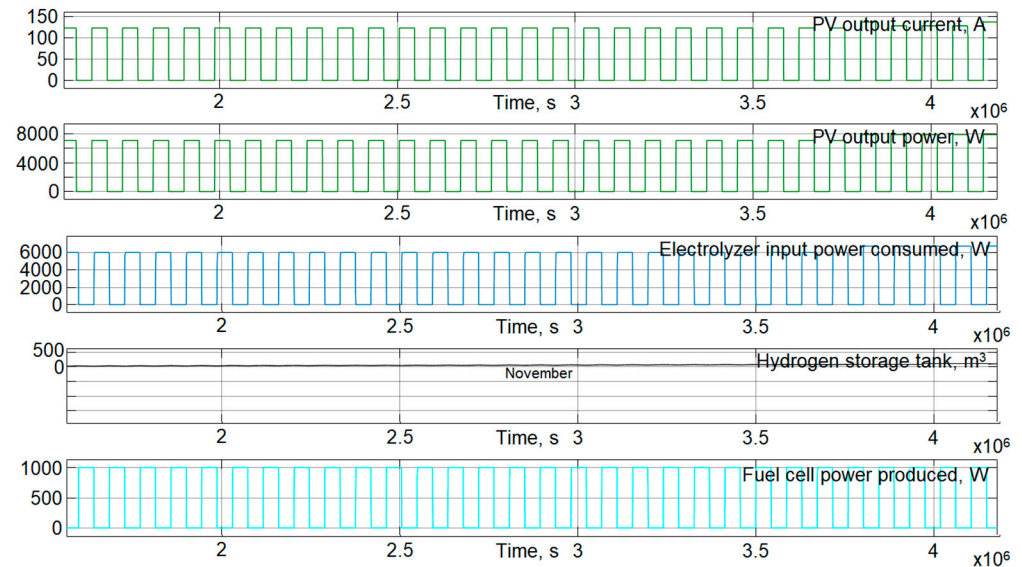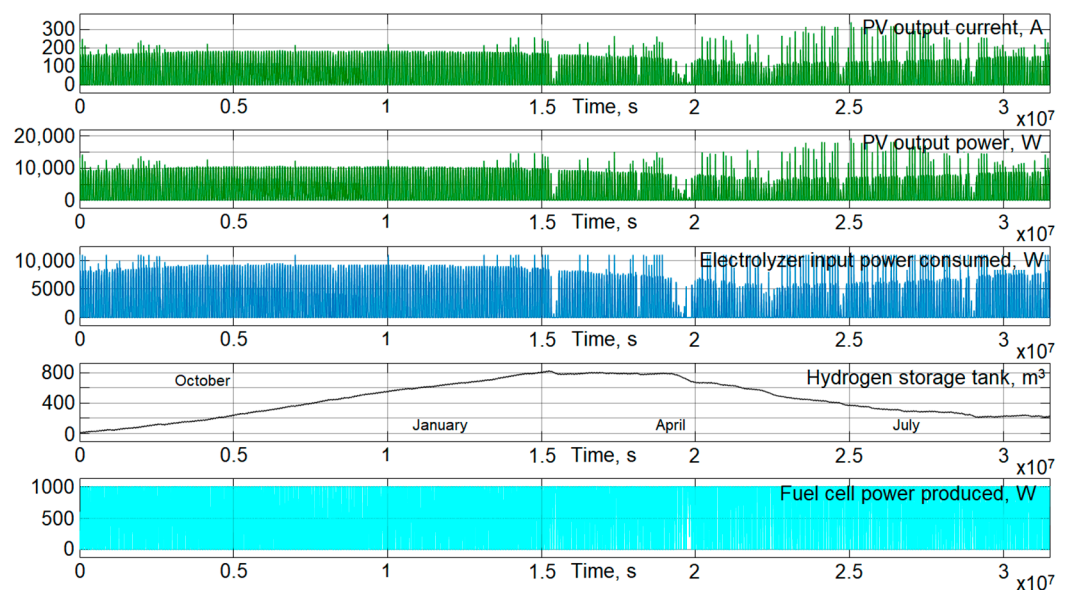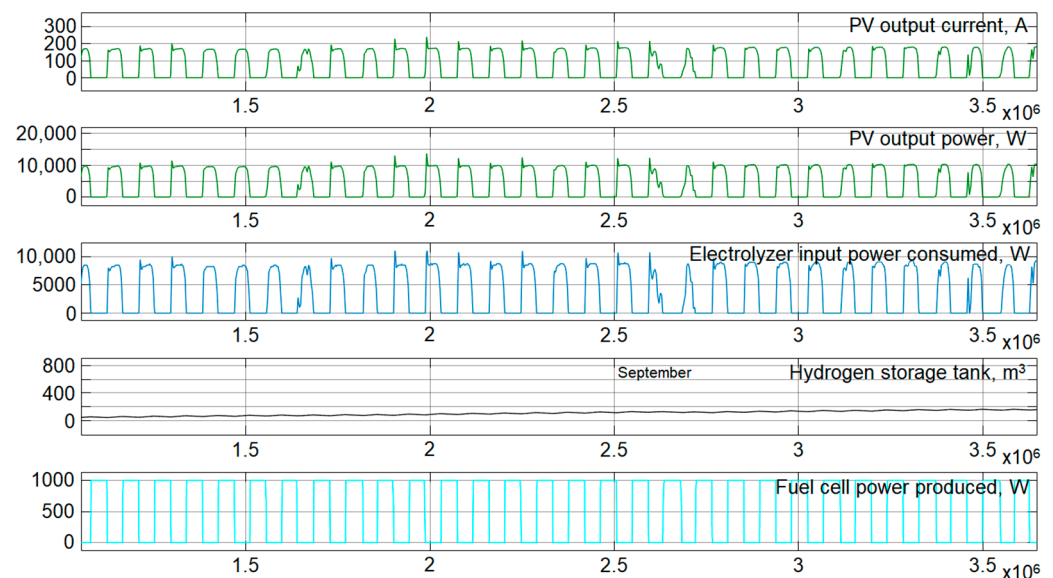

Figure 22. The result of the simulation and calculation of the required hydrogen tank capacity for the location Gnaraloo, Australia (April only).

4. Results

4.1. Results of Simulation

The analysis shows the following results:

- The solar-powered hydrogen uninterrupted power plant in Australia requires 1.5 times fewer solar modules (23 pcs) for supplying the same 1 kW power consumer than it would require for Russia (35 pcs).
- The hydrogen storage tank for Russia is almost twice as large as that for Australia and three times more than that for India, owing to more constant insolation in Manipal.
- The electrolyzer power consumption also differs from location to location and reflects the time of its operation. In Russia, it works less; however, more solar modules should be used to drive it.

4.2. Results of Optimizing

The optimization of the solar modules number in array leads to the optimization of the electrolyzer operation time and hydrogen storage tank volume. The higher and more plentiful the insolation, the fewer solar modules in an array and the shorter the operation time of the electrolyzer, which also means lower volume of the storage tank. The comparison results are presented in Table 4.

The simulation shows that the optimization does not influence the operating time and capacity of the fuel cell stack.

In general, the generating equipment (solar modules number) for the locations close to the Equator are of lesser capacity than others. At the same time, the hydrogen storage capacity does not differ much (three times higher in Russia than in India and two times

higher than in Australia). Metal organic based hydrogen storage can be applied to enhance storage capacity [58].

Table 4. Comparison of the optimized equipment components' capacities and time of electrolyzer operation.

Selected Location	Number of Solar Modules in an Array, pcs	Volume of Hydrogen Storage Tank, m^3	Total Energy Consumer by Electrolyzer per Year, kW·h
Chelyabinsk, Russia	35	2000	68×10^6
Manipal, India	32	600	90×10^6
Gnaraloo, Australia	23	800	80×10^6

5. Conclusions

The exhaustion of fossil fuels will inevitably lead mankind to the global usage of renewable energy sources, which will have to be developed in the sufficient quantities in about 30 years from now before oil and gas will run out. As renewables have the intermittent behavior, the hydrogen storage becomes one of the important areas for engineering development and, among all types of energy storage. It is considered as the mainstream direction to be realized before the hydrocarbons' apocalypse.

It is interesting how the solar generation and hydrogen storage equipment capacity parameters change from country to country and from one geographical location to another. To demonstrate the difference between location capabilities, three locations were selected in this study: Russia (as a country in the Northern Hemisphere), India (as a country near the Equator), and Australia (as the symmetrical country with India relative to the Equator, but in the Southern Hemisphere).

The study was based on the simulation in Matlab/Simulink with the conversion of power into electrical energy using the optimized number of solar modules and further generation of hydrogen gas by storing it in the tank. The main objective was to determine the optimal number of solar modules and maximal volume of hydrogen tank required, considering the same power consumption in each location.

The results obtained during the research are considered to be preliminary with much more analysis is needed in future. The comparison of the solar power capacity depending on the geographical location for the same hydrogen loop cycle equipment and identical consumption demonstrates the ability to use the unified solar, hydrogen, and fuel cell power generating equipment, and the results shows the difference between the solar module number, electrolyzer operating time, and maximal capacity of hydrogen storage tank depending on the insolation intensity.

The difference between location capabilities is rather considerable. Having the same consuming characteristics (1 kW power constant consumption), the power plant in Russia would require 35 solar modules against 23 in Australia and a three times bigger hydrogen tank. In India, almost the same number of solar modules (32) as in Russia (35) which makes it possible to reduce the hydrogen tank twofold. However, in terms of hydrogen equipment capacity, there is small difference between India and Australia, but there is large difference in terms of solar modules—32 against 23. This indicates that there is better insolation in Australia, notwithstanding that the points are located at almost similar latitudes, but on different sides of the equator. The study shows that the appropriate financial expenses on the same power consumption/generation in Australia will be 1.5 times less than in India and almost 3 times less than in Russia. This in turn means that, in general, business and residence expenses will be comparable.

Further research will be devoted in optimizing the solar modules number, hydrogen tank capacity, and electrolyzer operating time in automatic duty cycles, using the same Matlab/Simulink, but with automated optimized conditions. Several other locations are to be selected for comparison purposes (North and South America, Africa, China, areas closed to the North and South Poles, and so on). Moreover, the authors have an idea of building an interactive calculator of the required solar array, power of electrolyzer, fuel cell stack,

and hydrogen tank volume, depending on geographical location and power consumption graphs. The separate research area would be an extension of the experimental activity in the Arctic where the authors installed the wind-powered hydrogen equipment in 2013.

Author Contributions: Conceptualization, E.S.; Data curation, S.P.S., and S.K.; Formal analysis, E.S., and S.P.S.; Investigation, S.P.S., and A.K.; Methodology, E.S., and S.P.S.; Project administration, E.S., and S.P.S.; Resources, S.P.S., and S.K.; Supervision, E.S.; Validation, S.K. and S.P.S.; Visualization, E.S., and S.P.S.; Writing—original draft, E.S., and A.K.; Writing—review & editing, E.S., S.K., R.M.S., and S.P.S. All of the authors contributed significantly to the completion of this manuscript, conceiving and designing the research, and writing and improving the paper. All authors have read and agreed to the published version of the manuscript.

Conflicts of Interest: The authors declare no conflict of interest.

References

1. Ramyashree, M.S.; Priya, S.S.; Freudenberg, N.C.; Sudhakar, K.; Tahir, M. Metal-organic framework-based photocatalysts for carbon dioxide reduction to methanol: A review on progress and application. *J. CO2 Util* **2020**, *43*, 101374.
2. Gamil, M.M.; Sugimura, M.; Nakadomari, A.; Senjyu, T.; Howlader, H.O.R.; Takahashi, H.; Hemeida, A.M. Optimal Sizing of a Real Remote Japanese Microgrid with Sea Water Electrolysis Plant Under Time-Based Demand Response Programs. *Energies* **2020**, *13*, 3666. [CrossRef]
3. Saiprasad, N.; Kalam, A.; Zayegh, A. Triple Bottom Line Analysis and Optimum Sizing of Renewable Energy Using Improved Hybrid Optimization Employing the Genetic Algorithm: A Case Study from India. *Energies* **2019**, *12*, 349. [CrossRef]
4. Variar, A.G.; Ramyashree, M.S.; Ail, V.U.; Priya, S.S.; Sudhakar, K.; Tahir, M. Influence of various operational parameters in enhancing photocatalytic reduction efficiency of carbon dioxide in a photoreactor: A Review. *J. Ind. Eng. Chem.* **2021**. [CrossRef]
5. Our World in Data. Fossil Fuels, (n.d.). Available online: https://ourworldindata.org/fossil-fuels (accessed on 25 April 2021).
6. Oil Reserves. BP. 2021, (n.d.). Available online: https://www.bp.com/en/global/corporate/energy-economics/statistical-review-of-world-energy/oil.html (accessed on 25 April 2021).
7. Martins, F.; Felgueiras, C.; Smitkova, M.; Caetano, N. Analysis of Fossil Fuel Energy Consumption and Environmental Impacts in European Countries. *Energies* **2019**, *12*, 964. [CrossRef]
8. China, D. Fueling the Future of Mobility Hydrogen and fuel cell solutions for transportation. *Financ. Advis.* **2020**, *1*. Available online: https://www2.deloitte.com/content/dam/Deloitte/cn/Documents/finance/deloitte-cn-fueling-the-future-of-mobility-en-200101.pdf (accessed on 7 January 2021).
9. Gurtner, B. The Financial and Economic Crisis and Developing Countries. *Int. Dev. Policy, Rev. Int. Polit. Développement* **2010**, *1*, 189–213. [CrossRef]
10. BP Energy Outlook. Edition The Energy Outlook Explores the Forces Shaping the Global Energy Transition Out to 2040 and the Key Uncertainties Surrounding That; BP Energy Outlook, London, United Kingdom.: 2019. Available online: www.bp.com (accessed on 25 April 2021).
11. Bethoux, O. Hydrogen Fuel Cell Road Vehicles and Their Infrastructure: An Option towards an Environmentally Friendly Energy Transition. *Energies* **2020**, *13*, 6132. [CrossRef]
12. Felseghi, R.-A.; Carcadea, E.; Raboaca, M.S.; Trufin, C.N.; Filote, C. Hydrogen Fuel Cell Technology for the Sustainable Future of Stationary Applications. *Energies* **2019**, *12*, 4593. [CrossRef]
13. Rosen, M.A.; Koohi-Fayegh, S. The prospects for hydrogen as an energy carrier: An overview of hydrogen energy and hydrogen energy systems. *Energy Ecol. Environ.* **2016**, *1*, 10–29. [CrossRef]
14. Azni, M.; Khalid, R.M. Hydrogen Fuel Cell Legal Framework in the United States, Germany, and South Korea—A Model for a Regulation in Malaysia. *Sustainability* **2021**, *13*, 2214. [CrossRef]
15. Kwon, H.-I.; Cho, Y.-S.; Choi, S.-M. A Study on Optimal Power System Reinforcement Measures Following Renewable Energy Expansion. *Energies* **2020**, *13*, 5929. [CrossRef]
16. Kumar, G.V.; Sarojini, R.K.; Palanisamy, K.; Padmanaban, S.; Holm-Nielsen, J.B. Large Scale Renewable Energy Integration: Issues and Solutions. *Energies* **2019**, *12*, 1996. [CrossRef]
17. Jiménez-Buendía, F.; Villena-Ruiz, R.; Honrubia-Escribano, A.; Molina-García, Á.; Gómez-Lázaro, E. Submission of a WECC DFIG Wind Turbine Model to Spanish Operation Procedure 12.3. *Energies* **2019**, *12*, 3749. [CrossRef]
18. Méndez, C.; Bicer, Y. Qatar's Wind Energy Potential with Associated Financial and Environmental Benefits for the Natural Gas Industry. *Energies* **2019**, *12*, 3329. [CrossRef]

19. Francis, A.; Priya, S.S.; Kumar, S.H.; Sudhakar, K.; Tahir, M. A review on recent developments in solar photoreactors for carbon dioxide conversion to fuels. *J. CO2 Util* **2021**, *47*, 101515. [CrossRef]

20. Daraei, M.; Campana, P.E.; Thorin, E. Power-to-hydrogen storage integrated with rooftop photovoltaic systems and combined heat and power plants. *Appl. Energy* **2020**, *276*, 115499. [CrossRef]

21. Hofmann, F.; Schlott, M.; Kies, A.; Stöcker, H. Flow Allocation in Meshed AC-DC Electricity Grids. *Energies* **2020**, *13*, 1233. [CrossRef]

22. Al Wahedi, A.; Bicer, Y. A Case Study in Qatar for Optimal Energy Management of an Autonomous Electric Vehicle Fast Charging Station with Multiple Renewable Energy and Storage Systems. *Energies* **2020**, *13*, 5095. [CrossRef]

23. Bizon, N.; Stan, V.A.; Cormos, A.C. Stan Optimization of the Fuel Cell Renewable Hybrid Power System using the Control Mode of the Required Load Power on the DC Bus. *Energies* **2019**, *12*, 1889. [CrossRef]

24. Bajan, B.; Łukasiewicz, J.; Poczta-Wajda, A.; Poczta, W. Edible Energy Production and Energy Return on Investment—Long-Term Analysis of Global Changes. *Energies* **2021**, *14*, 1011. [CrossRef]

25. Morenov, V.; Leusheva, E.; Buslaev, G.; Gudmestad, O.T. System of Comprehensive Energy-Efficient Utilization of Associated Petroleum Gas with Reduced Carbon Footprint in the Field Conditions. *Energies* **2020**, *13*, 4921. [CrossRef]

26. Pijarski, P.; Kacejko, P. Voltage Optimization in MV Network with Distributed Generation Using Power Consumption Control in Electrolysis Installations. *Energies* **2021**, *14*, 993. [CrossRef]

27. Węcel, D.; Jurczyk, M.; Uchman, W.; Skorek-Osikowska, A. Investigation on System for Renewable Electricity Storage in Small Scale Integrating Photovoltaics, Batteries, and Hydrogen Generator. *Energies* **2020**, *13*, 6039. [CrossRef]

28. Ostadi, M.; Paso, K.G.; Rodriguez-Fabia, S.; Øi, L.E.; Manenti, F.; Hillestad, M. Process Integration of Green Hydrogen: Decarbonization of Chemical Industries. *Energies* **2020**, *13*, 4859. [CrossRef]

29. Szima, S.; Cormos, C.-C. CO_2 Utilization Technologies: A Techno-Economic Analysis for Synthetic Natural Gas Production. *Energies* **2021**, *14*, 1258. [CrossRef]

30. Qyyum, M.A.; Chaniago, Y.D.; Ali, W.; Saulat, H.; Lee, M. Membrane-Assisted Removal of Hydrogen and Nitrogen from Synthetic Natural Gas for Energy-Efficient Liquefaction. *Energies* **2020**, *13*, 5023. [CrossRef]

31. Lahnaoui, A.; Wulf, C.; Dalmazzone, D. Optimization of Hydrogen Cost and Transport Technology in France and Germany for Various Production and Demand Scenarios. *Energies* **2021**, *14*, 744. [CrossRef]

32. Hinokuma, T.; Farzaneh, H.; Shaqour, A. Techno-Economic Analysis of a Fuzzy Logic Control Based Hybrid Renewable Energy System to Power a University Campus in Japan. *Energies* **2021**, *14*, 1960. [CrossRef]

33. Mun, H.; Moon, B.; Park, S.; Yoon, Y. A Study on the Economic Feasibility of Stand-Alone Microgrid for Carbon-Free Island in Korea. *Energies* **2021**, *14*, 1913. [CrossRef]

34. Abas, N.; Kalair, A.; Khan, N. Review of fossil fuels and future energy technologies. *Futures* **2015**, *69*, 31–49. [CrossRef]

35. Gül, M.; Akyüz, E. Hydrogen Generation from a Small-Scale Solar Photovoltaic Thermal (PV/T) Electrolyzer System: Numerical Model and Experimental Verification. *Energies* **2020**, *13*. [CrossRef]

36. Choi, H.-U.; Choi, K.-H. Performance Evaluation of PV/T Air Collector Having a Single-Pass Double-Flow Air Channel and Non-Uniform Cross-Section Transverse Rib. *Energies* **2020**, *13*, 2203. [CrossRef]

37. Kim, J.-H.; Ahn, J.-G.; Kim, J.-T. Demonstration of the Performance of an Air-Type Photovoltaic Thermal (PVT) System Coupled with a Heat-Recovery Ventilator. *Energies* **2016**, *9*, 728. [CrossRef]

38. Calise, F.; Figaj, R.D.; Vanoli, L. Experimental and Numerical Analyses of a Flat Plate Photovoltaic/Thermal Solar Collector. *Energies* **2017**, *10*, 491. [CrossRef]

39. Yi, T.; Tong, L.; Qiu, M.; Liu, J. Analysis of Driving Factors of Photovoltaic Power Generation Efficiency: A Case Study in China. *Energies* **2019**, *12*, 355. [CrossRef]

40. Nespoli, A.; Ogliari, E.; Leva, S.; Pavan, A.M.; Mellit, A.; Lughi, V.; Dolara, A. Day-Ahead Photovoltaic Forecasting: A Comparison of the Most Effective Techniques. *Energies* **2019**, *12*, 1621. [CrossRef]

41. Li, W.; Ren, H.; Chen, P.; Wang, Y.; Qi, H. Key Operational Issues on the Integration of Large-Scale Solar Power Generation—A Literature Review. *Energies* **2020**, *13*, 5951. [CrossRef]

42. Dolara, A.; Grimaccia, F.; Leva, S.; Mussetta, M.; Ogliari, E. A Physical Hybrid Artificial Neural Network for Short Term Forecasting of PV Plant Power Output. *Energies* **2015**, *8*, 1138–1153. [CrossRef]

43. Massucco, S.; Mosaico, G.; Saviozzi, M.; Silvestro, F. A Hybrid Technique for Day-Ahead PV Generation Forecasting Using Clear-Sky Models or Ensemble of Artificial Neural Networks According to a Decision Tree Approach. *Energies* **2019**, *12*, 1298. [CrossRef]

44. Al-Dahidi, S.; Ayadi, O.; Adeeb, J.; Alrbai, M.; Qawasmeh, B.R. Extreme Learning Machines for Solar Photovoltaic Power Predictions. *Energies* **2018**, *11*, 2725. [CrossRef]

45. Liu, W.; Liu, C.; Lin, Y.; Ma, L.; Xiong, F.; Li, J. Ultra-Short-Term Forecast of Photovoltaic Output Power under Fog and Haze Weather. *Energies* **2018**, *11*, 528. [CrossRef]

46. Lee, D.; Kim, K. Recurrent Neural Network-Based Hourly Prediction of Photovoltaic Power Output Using Meteorological Information. *Energies* **2019**, *12*, 215. [CrossRef]

47. Machlev, R.; Batushansky, Z.; Soni, S.; Chadliev, V.; Belikov, J.; Levron, Y. Verification of Utility-Scale Solar Photovoltaic Plant Models for Dynamic Studies of Transmission Networks. *Energies* **2020**, *13*, 3191. [CrossRef]

48. Schouten, B. Thermal efficiency Improvement of Closed Hydrogen and Oxygen Fuelled Combined Cycle Power Plants with the Application of Solid Oxide Fuel Cells Using an Exergy Analysis Method. Master's Thesis, Delft University of Technology, Delft, The Netherlands, 9 April 2020.

49. Tables of Monthly and Annual Amounts of Total Solar Radiation. Russian Region., NASA. (n.d.). Available online: https://www.solarhome.ru/basics/solar/radiation.htm (accessed on 9 April 2021).

50. Photovoltaic Geographical Information System, Eur. Comm. (n.d.). Available online: https://re.jrc.ec.europa.eu/pvg_tools/en/tools.html (accessed on 9 April 2021).

51. Pombeiro, H.; Silva, C.S. Analyzing Residential Electricity Consumption Patterns Based on Consumer's Segmentation. 2012. Available online: http://ceur-ws.org/Vol-923/paper05.pdf (accessed on 25 April 2021).

52. Hobby, J.D.; Tucci, G.H. Analysis of the residential, commercial and industrial electricity consumption. In Proceedings of the 2011 IEEE PES Innovative Smart Grid Technologies, Perth, WA, Australia, 13–16 November 2011; pp. 1–7. [CrossRef]

53. Parameters of Solar Module, (n.d.). Available online: https://www.hevelsolar.com/catalog/solnechnye-moduli/ (accessed on 9 April 2021).

54. VOLTIANA Electrolyzer. Technical Documentation. H2Nitidor Company, (n.d.). Available online: www.h2nitidor.com (accessed on 5 March 2021).

55. Ultra-light Fuel Stack AEROSTAK Horizon, (n.d.). Available online: http://new.novatorlab.ru/ru/katalog/promyshlennost/toplivnye-elementy/ultralegkij-toplivnyj-stek-aerostaks-horizon-1000-vt (accessed on 5 March 2021).

56. Table: Hydrogen Density at Different Temperatures and Pressures, Hydrog. Tools. (n.d.). Available online: https://h2tools.org/hyarc/hydrogen-data/hydrogen-density-different-temperatures-and-pressures (accessed on 25 April 2021).

57. Solomin, E.; Kirpichnikova, I.; Amerkhanov, R.; Korobatov, D.; Lutovats, M.; Martyanov, A. Wind-hydrogen standalone uninterrupted power supply plant for all-climate application. *Int. J. Hydrogen Energy* **2019**, *44*, 3433–3449. [CrossRef]

58. Shet, S.P.; Priya, S.S.; Sudhakar, K.; Tahir, M. A review on current trends in potential use of metal-organic framework for hydrogen storage. *Int. J. Hydrogen Energy* **2021**, *46*, 11782–11803. [CrossRef]